



Gastric sub-epithelial tumors: identification of gastrointestinal stromal tumors using CT with a practical scoring method

Ming Liu¹ · Liheng Liu² · Erhu Jin³

Received: 16 October 2018 / Accepted: 26 November 2018 / Published online: 9 December 2018
© The International Gastric Cancer Association and The Japanese Gastric Cancer Association 2018

Abstract

Objectives To determine CT features that can identify gastrointestinal stromal tumors (GISTs) among gastric sub-epithelial tumors (SETs) and to explore a practical scoring method.

Methods Sixty-four patients with gastric SETs (51 GISTs and 13 non-GISTs) from hospital I were included for primary analyses, and 92 (67 GISTs and 25 non-GISTs) from hospital II constituted a validation cohort. Pre-operative CT images were reviewed for imaging features: lesion location, growth pattern, lesion margin, enhancement pattern, dynamic pattern, attenuation at each phasic images and presence of necrosis, superficial ulcer, calcification, and peri-lesion enlarged lymph node (LN). Clinical and CT features were compared between the two groups (GISTs versus non-GISTs) and a GIST-risk scoring method was developed; then, its performance for identifying GISTs was tested in the validation cohort.

Results Seven clinical and CT features were significantly suggestive of GISTs rather than non-GISTs: older age (> 49 years), non-cardial location, irregular margin, lower attenuation on unenhanced images (≤ 43 HU), heterogeneous enhancement, necrosis, and absence of enlarged LN ($p < 0.05$). At validation step, the established scoring method with cut-off score dichotomized into ≥ 4 versus < 4 for identifying GISTs revealed an AUC of 0.97 with an accuracy of 92%, a sensitivity of 100% and a negative predictive value (NPV) of 100%.

Conclusions Gastric GISTs have special CT and clinical features that differ from non-GISTs. With a simple and practical scoring method based on the significant features, GISTs can be accurately differentiated from non-GISTs.

Keywords Tomography · X-ray computed · Stomach · Neoplasms · Gastrointestinal stromal tumors · Diagnosis

Abbreviations

SETs	Sub-epithelial tumors
GISTs	Gastrointestinal stromal tumors
AP	Arterial phase
VP	Venous phase
DP	Delayed phase
HU	Housefield unit
LN	Lymph node

Introduction

Gastrointestinal stromal tumors (GISTs) of stomach represent a distinct histopathologic group of sub-epithelial tumors (SETs) that are increasingly encountered during gastrointestinal tract diseases screening. Meanwhile, a wide range of mesenchymal neoplasms other than GISTs (non-GISTs) can also originate in stomach and usually present similar imaging features, sometimes even similar pathologic morphological manifestation with GISTs [1]. However, the prognosis and management of the two groups extremely differed. Curative surgical resection is required for cure of gastric GISTs due to the high malignant potentials [2, 3]. In contrast, almost all gastric non-GISTs SETs, mainly consist of leiomyoma and schwannoma [4, 5], are benign and remain stable [4], so conservative medical management or less-invasive resection approach is usually recommended and performed [6, 7]. Therefore, the accurate pre-operative differentiation of gastric GISTs from non-GISTs is of great importance for patients care and decision making [8].

✉ Liheng Liu
liu.liheng@zs-hospital.sh.cn

¹ Department of Radiotherapy, Fudan University Shanghai Cancer Center, Shanghai, China

² Department of Radiology, Zhongshan Hospital, Fudan University, No. 180 Fenglin Road, Xuhui District, Shanghai 200032, China

³ Department of Radiology, Beijing Friendship Hospital, Capital Medical University, Beijing, China

Endoscopic biopsy can be used for pre-operative evaluation of SETs of stomach, but it usually cannot give a reliable diagnosis, and definitive diagnosis needs immunohistochemical staining which should be obtained after surgical resection. Recently, CT has been considered to have different advantages for the pre-operative diagnosis of gastric SETs [8, 9]. By using CT to evaluate the attenuation value, enhancement pattern, and other morphologic features, it is possible to generate a conclusive diagnosis and predict the malignancy [8]. Choi et al. [10] utilized CT to differentiate large (≥ 5 cm) gastric GISTs from benign SETs and obtained a positive result (diagnostic accuracy 87–90%). However, majority of gastric SETs are initially detected with a small diameter of < 5 cm (45% of GISTs and 60–75% of benign SETs) and are also challenging to manage due to lack of symptom and unclear biological behavior [11–13]. Therefore, identifying GISTs among both large and small sizes of gastric SETs may be more clinically important.

Thus, the purposes of this study are: (1) to determine significant CT features that could help to identify GISTs among gastric SETs and (2) to explore a practical scoring method based on combination of the significant features and to evaluate its diagnostic performance.

Methods

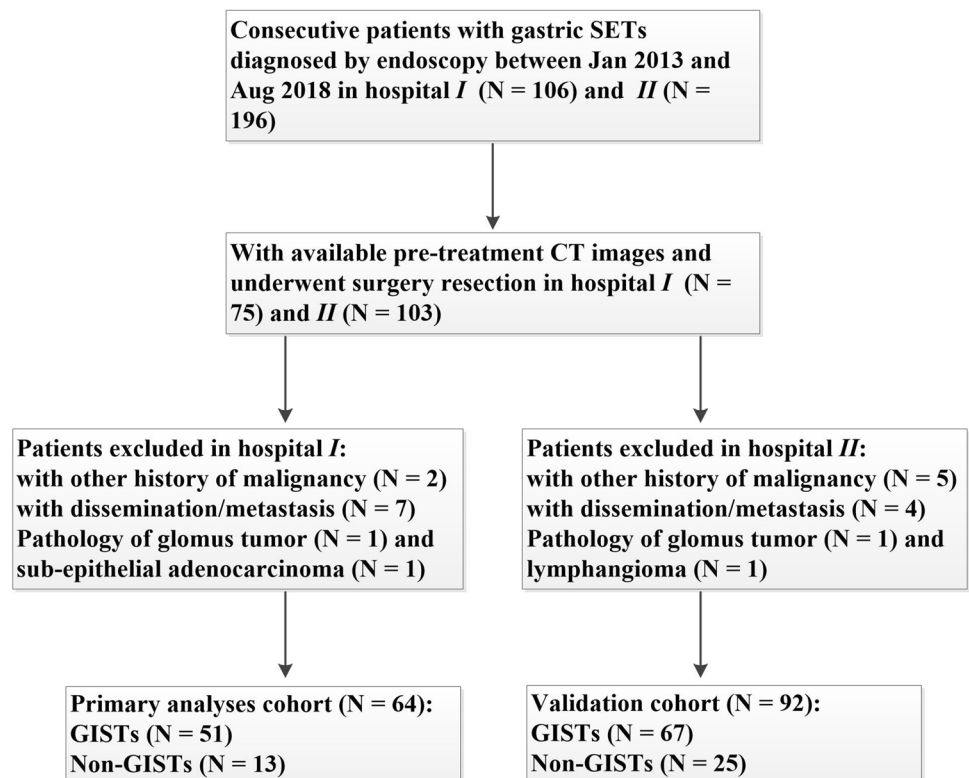
Our study population was obtained from two independent hospitals. The primary analyses cohort from hospital I was investigated to determine significant CT features and explore a practical scoring method for distinguishing GISTs from non-GISTs; subsequently, patients from hospital II constituted an external validation cohort to test the performance of the scoring method. This study was approved by local institutional review board from both hospitals and informed consent was waived according to the retrospective design.

Patients

Medical record of both hospitals between January 2013 and August 2018 was reviewed. For study inclusion: (1) patients who diagnosed with gastric SETs by endoscopy; (2) with pre-treatment gastric CT imaging (pre- and post-enhanced scans) available for analysis; and (3) underwent surgical resection (laparoscopic, endo-luminal or open surgery) and with definite histopathological results. Exclusion criteria were: (1) with other history of malignancy; (2) underwent any treatment before CT scan; and (3) with obvious disseminated or metastatic lesion at primary imaging.

First, 106 consecutive patients with endoscopy-diagnosed gastric SETs were initially identified from hospital I, of which 75 patients met the inclusion criteria (Fig. 1).

Fig. 1 Flowchart showing the inclusion process of primary analyses and validation cohort. SETs sub-epithelial tumors, GISTs gastrointestinal stromal tumors



Nine patients were excluded because of coexisting gastric carcinoma ($N=2$) or with peritoneal dissemination or/and liver metastatic lesion ($N=7$). In addition, two patients with pathologic diagnosis of glomus tumor and sub-epithelial adenocarcinoma were excluded because of straightforward enhanced-CT manifestation or non-mesenchymal origin. Finally, 64 patients with gastric SETs were included from hospital I for primary analyses step of the study: 51 patients with GISTs and 13 with non-GISTs (seven with leiomyoma and six with schwannoma). Study population characteristics are listed in Table 1.

Second, 196 consecutive patients were initially identified in hospital II, and 103 of them met the inclusion criteria (Fig. 1). Nine patients were excluded due to with other history of malignancy ($N=5$) or with peritoneal dissemination or/and liver metastatic lesion ($N=4$). Similarly, patients with

sub-epithelial lymphangioma ($N=1$) and glomus ($N=1$) were excluded because of straightforward imaging features. Finally, 92 patients were included from hospital II and constituted a validation data set for the scoring method: 67 patients with GISTs and 25 non-GISTs (ten with leiomyoma, one with inflammatory polyp, and 14 with schwannoma).

CT imaging acquisition

Multi-phasic contrast-enhanced-CT scans were performed using multi-detector CT scanner (Brilliance 128, Philips, Best, The Netherlands, Somatom sensation 64, Siemens, Erlangen, Germany or Aquilion one 320, Toshiba, Tokyo, Japan) in patients who had fasted more than 8 h. To achieve gastric distention, 600–800 ml tap water was ingested before CT examination. Scan parameters were collimation

Table 1 Clinical and imaging features' distribution between groups of GISTs and non-GISTs of the primary analyses cohort

	GISTs ($N=51$)	Non-GISTs ($N=13$)			<i>p</i> value
		Leiomyoma ($N=7$)	Schwannoma ($N=6$)	Non-GISTs (leiomyoma + schwannoma)	
Age, years (range)	60.1 (15–83)	40.1 (29–46)	49.6 (32–71)	44.5 (29–71)	0.001
Gender, <i>n</i> (%)					0.489
Male	29 (56.9%)	3 (42.9%)	3 (50%)	6 (46.1%)	
Female	22 (43.1%)	4 (57.1%)	3 (50%)	7 (53.9%)	
Location, <i>n</i> (%)					<0.001
Cardia	0 (0%)	6 (85.7%)	0 (0%)	6 (46.2%)	
Fundus	24 (47.1%)	0 (0%)	1 (16.7%)	1 (7.7%)	
Body	20 (39.2%)	1 (14.3%)	5 (83.3%)	6 (46.2%)	
Antrum	7 (13.7%)	0 (0%)	0 (0%)	0 (0%)	
Growth pattern, <i>n</i> (%)					0.827
Endophytic	27 (52.9%)	5 (71.4%)	3 (50%)	8 (61.5%)	
Exophytic	16 (31.4%)	1 (14.3%)	2 (33.3%)	3 (23.1%)	
Mixed	8 (15.7%)	1 (14.3%)	1 (16.7%)	2 (15.4%)	
Margin, <i>n</i> (%)					<0.001
Smooth	12 (23.5%)	7 (100%)	6 (100%)	13 (100%)	
Irregular	39 (76.5%)	0 (0%)	0 (0%)	0 (0%)	
Size, cm, mean (range)	3.5 (1.2–16) ^a	2.3 (1.3–4.3)	4.7 (2.8–7.0)	3.4 (1.3–7.0)	0.263
NE attenuation, HU, mean (range)	33.3 (24–45)	39.4 (27–50)	45.3 (33–57)	42.2 (27–57)	0.003
AP attenuation, HU, mean (range)	47.4 (29–71)	49.7 (43–56)	54.5 (36–66)	51.9 (36–66)	0.145
VP attenuation, HU, mean (range)	59.1 (35–82)	59.3 (41–101)	65.8 (47–85)	62.3 (41–101)	0.441
DP attenuation, HU, mean (range)	64.3 (35–92)	68.4 (56–94)	72.3 (51–90)	70.2 (51–94)	0.168
Heterogeneous on VP, <i>n</i> (%)	33 (64.7%)	1 (14.3%)	1 (16.7%)	2 (15.3%)	<0.001
Superficial ulcer, <i>n</i> (%)	11 (21.6%)	0 (0%)	1 (16.7%)	1 (7.7%)	0.253
Calcification, <i>n</i> (%)	11 (21.6%)	1 (14.3%)	3 (50%)	4 (30.8%)	0.485
Necrosis, <i>n</i> (%)	25 (49%)	0 (0%)	1 (16.7%)	1 (7.7%)	0.007
Peri-lesion enlarged LN, <i>n</i> (%)	0 (0%)	0 (0%)	4 (67%)	4 (30.7%)	<0.001

GISTs gastrointestinal stromal tumors, NE non-enhanced, AP arterial phase, VP venous phase, DP delayed phase, HU housefield unit, LN lymph node

^aNon-normal distribution data, expressed as median (range)

of 0.625–1 mm, gantry rotation time of 0.5–0.75 s, 120 kV and 250 mAs. Contrast-enhanced scanning was conducted after a bolus intravenous injection of 1.5 ml/kg of non-ionic contrast agent (Ultravist 350, Bayer healthcare, Berlin, Germany) followed by 30 ml saline flush at a rate of 3 ml/s. Scans were started at 6 s (arterial phase), 46 s (venous phase), and 96 s (delayed phase) after a trigger threshold of 100 Hounsfield unit (HU) was reached at abdominal aorta. All images were reconstructed with slice thickness/interval of not thicker than 5 mm for clinical analysis.

Image interpretation

CT images were reviewed retrospectively and independently by two gastrointestinal radiologists (A, with 12 years of experience, and B with 9 years of experience), who knew that patients had gastric sub-epithelial lesions, but were unaware of any other clinical or surgical data. When discrepancy existed between the two radiologists' diagnoses, the final result was decided according to their consensus. Before reading, the radiologists received training in recognizing the involved CT features: lesion location (cardia, fundus, body, or antrum of stomach), growth pattern (endophytic, exophytic, or mixed), lesion margin (smooth or irregular), attenuation value at each phase, enhancement pattern (homogeneous or heterogeneous on venous phase images), dynamic pattern (progressive enhancement or other) and presence of necrosis, superficial ulcer, calcification, and enlarged perilesion lymph node (LN). Necrosis was considered present when non-enhancing or cystic area was observed within the tumor. Superficial ulcer was defined as focal tissue defect existing at the surface of the tumor [10]. An LN over 6 mm (short-axis diameter) was considered as LN enlargement. When measuring attenuation value of each tumor, an oval or round region of interest (ROI, larger than 10 mm²) was drawn on the non-necrotic zone while avoiding the calcification if exist, then was copied to the other phases of images. The dynamic pattern of enhancement was defined according to the attenuation value through different phases of each mass, as follows: (1) progressive enhancement: the mass enhancing gradually and reaching maximal attenuation value at delayed phase and (2) other patterns: wash in/wash out or stable pattern [14].

Post-operative pathological analysis and diagnosis

Final diagnoses of all enrolled patients were established by the consensus of pathological profile and immunohistochemical (IHC) analysis after surgical resection of masses [2]. For IHC analysis, expression of c-KIT and CD34 and/or DOG1 is consistent with GISTs, positive reaction for desmin indicates leiomyoma and S-100 indicates schwannoma.

Statistical analysis

At primary analyses' step, for inter-observer agreement of CT features identifying and attenuation measuring, kappa and intra-class correlation coefficient (ICC) were calculated, respectively. To test differences of CT and clinical features between patients groups with GISTs or non-GISTs, the Student *t* or Mann–Whitney *U* test was performed for quantitative data and χ^2 or Fisher exact test was performed for categorical data. For significant quantitative data (radiologist A measured data were used at this step), receiver operating characteristic (ROC) curve was used to determine the best cut-off value to differentiate GISTs from non-GISTs (highest sum of specificity and sensitivity). After significant features were determined, a GIST-risk score was assigned to each patient according to the sum of significant features he had (add one point for each significant feature). The optimal cut-off point of the score was determined for distinguishing GISTs from begin non-GISTs at the first step.

At the validation step, the diagnostic of the established scoring method as well as the optimal cut-off point of score was tested on the data set derived from hospital II using ROC curve, and corresponding sensitivity and specificity were calculated.

All statistical analyses were performed using IBM SPSS Statistics for windows (V22.0, IBM corp, NY, USA). A value of $p < 0.05$ was considered to indicate a significant difference.

Results

Sixty-four patients from hospital I were included in the primary analyses cohort, and 92 patients from hospital II were included in the validation cohort.

Primary analyses

Inter-observer agreement

The inter-observer agreement for identification of all CT features was good to perfect with kappa values ranging from 0.742 to 0.931. Regarding measurement of attenuation at non-enhanced phase, agreement was also perfect with an ICC of 0.915.

Clinical and CT features between GIST and non-GIST groups

All features between GISTs and non-GISTs groups are summarized in Table 1. The mean age revealed a significant difference between groups with an optimal cut-off value of > 49 years for identifying GISTs (area under the ROC curve, AUC=0.86), and patients with gastric GISTs were much

older than those with non-GISTs (60.1 years versus 44.5 years, $p=0.001$). Of CT findings, distribution of tumor location significantly differed between groups, none of GISTs located at cardia of stomach, while nearly, half of non-GISTs did ($N=6$, 46.2%). Mean attenuation value on non-enhanced images was significantly lower in GISTs than that in non-GISTs (33.3 HU versus 42.2 HU, $p=0.003$) with an optimal cut-off value of ≤ 43 HU and an AUC of 0.78. In addition, irregular margin, heterogeneous enhancement, and necrosis were more frequently observed in GISTs, while peri-lesion LN enlargement was more common in non-GISTs. In terms of dynamic pattern of enhancement, both GISTs and non-GISTs demonstrated a progressive enhancement pattern (Fig. 2). No statistically significant differences were found for gender distribution, growth pattern, size, attenuation value on contrast-enhanced images, presence of superficial ulcer, or calcification between the two groups ($p > 0.05$).

SET-scoring method exploring

There were seven significant features that could be suggestive of GISTs rather than non-GISTs: older than 49 years, non-cardial location, irregular margin, lower attenuation on unenhanced images (≤ 43 HU), heterogeneous enhancement, necrosis, and absence of enlarged LN. Score of each patient was defined according to how many significant features he had. After scores for patients were all determined, we found

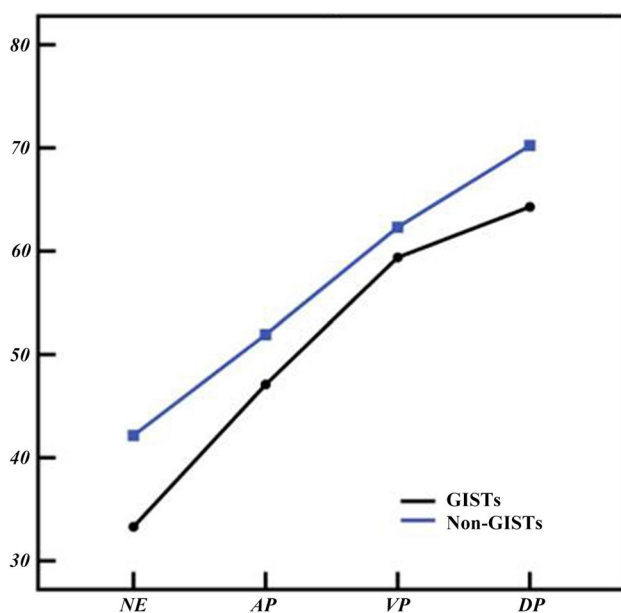


Fig. 2 Mean attenuation at different phases of CT images in primary analyses cohort. Both GISTs and non-GISTs demonstrated progressive enhancement pattern, and no significant difference was found between the two groups. *GISTs* gastrointestinal stromal tumors, *NE* non-enhanced phase, *AP* arterial phase, *VP* venous phase, *DP* delayed phase

that when the score was dichotomized into ≥ 4 versus < 4 , all GISTs and almost all non-GISTs were correctly identified, except for one case of schwannoma which was misdiagnosed as GISTs.

External validation

Validation of the established scoring method

Using the scoring method, all of 67 patients with GISTs in the validation cohort were accurately identified; meanwhile, seven of 25 non-GISTs were misdiagnosed as GISTs. The diagnostic accuracy of the scoring method for identifying GISTs revealed an AUC of 0.97 [95% confidence interval (CI) 0.91–0.99] when using the established cut-off score (≥ 4 versus < 4), it achieved an accuracy of 92% (95% CI 85–97), a sensitivity of 100% (95% CI 93–100), a specificity of 72% (95% CI 50–87), and a negative predictive value (NPV) of 100% (95% CI 78–100) (Fig. 3). Representative examples are illustrated in Figs. 4 and 5.

Discussion

In contrary to other gastric SETs, GISTs are almost always malignant, and even small lesions may show rapid disease progression and result in a high tumor-related mortality rate

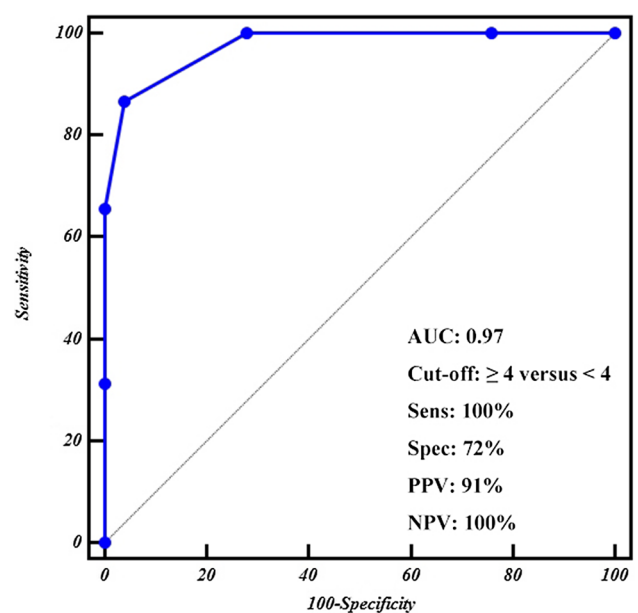


Fig. 3 Receiver operating characteristic curve of the scoring method for identifying GISTs. An AUC of 0.97 was revealed by the scoring method. An accuracy of 92%, a sensitivity of 100%, and a NPV of 100% were achieved when the established cut-off value (≥ 4 versus < 4) was used. *AUC* area under the curve, *Sens* sensitivity, *Spec* specificity, *PPV* positive predictive value, *NPV* negative predictive value

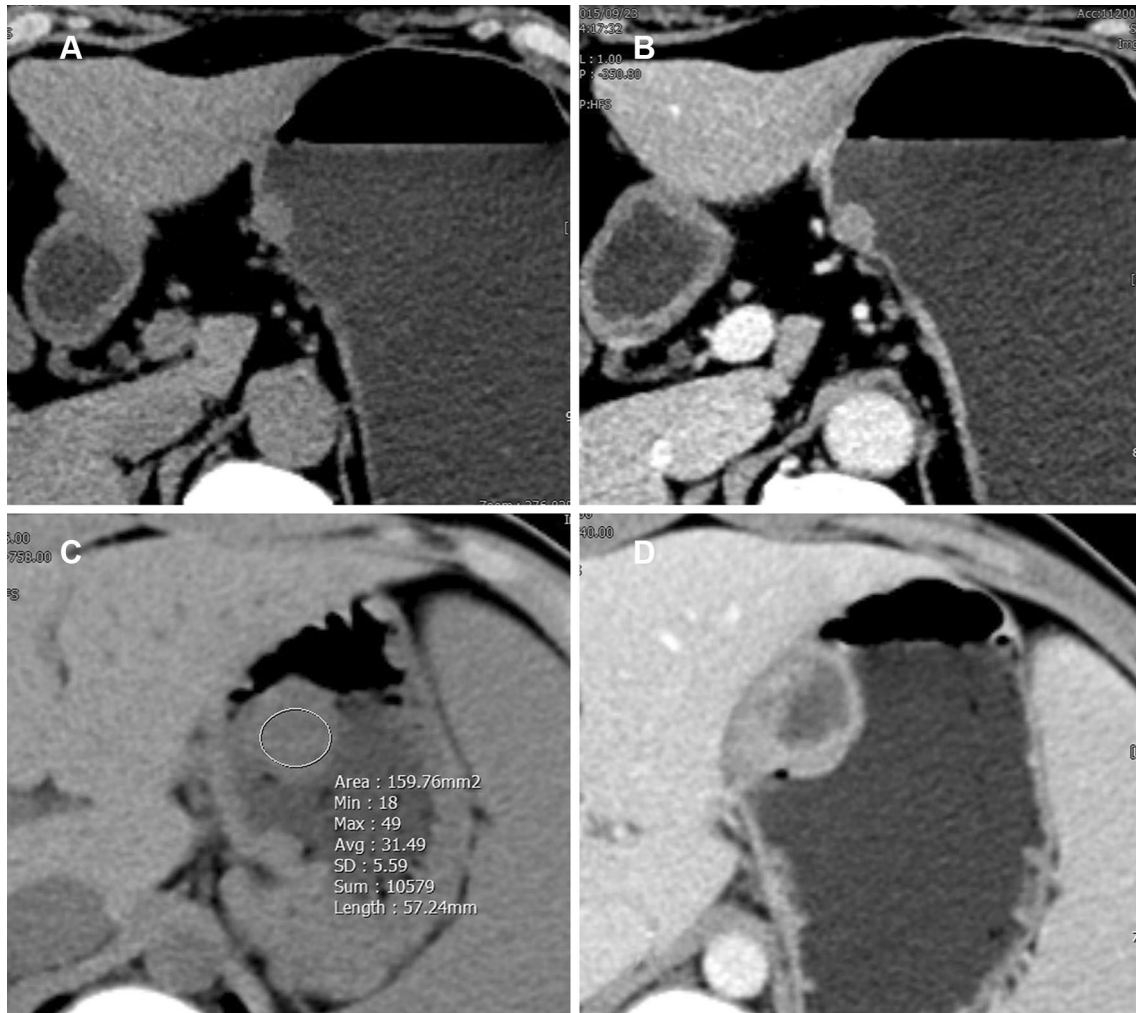


Fig. 4 **a, b** CT images of a 59-year-old (>49 years) woman with a 1.2 cm-sized sub-epithelial tumor. The lesion showing non-cardial location, irregular margin, lower attenuation on non-enhanced image (31 HU, < 43 HU) and absence of enlarged lymph node. A score of 5 was assigned. Postoperative pathological diagnosis is gastrointestinal stromal tumor (GIST). **c, d** CT images of a 15-year-old boy with

a 2.3 cm-sized sub-epithelial tumor. The lesion showing non-cardial location, irregular margin, lower attenuation on non-enhanced image (31 HU, < 43 HU), heterogeneous enhancement, presence of necrosis and absence of enlarged lymph node. A score of 6 was assigned. Postoperative pathological diagnosis is GIST

[15, 16]. Given the varied treatment principles and prognosis of gastric SETs, it is important to distinguish GISTs from non-GISTs before surgery. The present study demonstrated that CT and clinical features of non-cardial location, irregular margin, heterogeneous enhancement, lower attenuation on unenhanced images (≤ 43 HU), necrosis, absence of enlarged LN, and older age (> 49 years) could help to differentiate gastric GISTs from benign non-GISTs (leiomyoma and schwannoma). In addition, combination of these imaging and clinical features using a simple scoring method could obtain very high sensitivity and NPV for identification of GISTs.

Our study indicated that irregular margin, heterogeneous enhancement, and necrosis were more prevalent in gastric GISTs than in benign non-GISTs. Irregular

margin, which was considered caused by varied rates of tumor proliferation in different parts, has been shown to be associated with malignant behavior [17]. In our study, irregular margin more frequently appeared in GISTs even when with diameters less than 2.5 cm (Fig. 4). Heterogeneous enhancement and necrosis were believed result in the mismatching of neovascularization with quick growth rate in malignant tumor [15]. These three CT features may reflect the high level of intro-lesion heterogeneity in tumor with malignant potential, and are less likely to appear in benign lesion. In the primary analyses series, only two of the 13 non-GISTs showed heterogeneous enhancement, none showed irregular margin and one with intro-lesion necrosis. Similar results have been reported in the previous studies [10, 15, 18, 19]. In a research of application



Fig. 5 **a, b** CT images of a 29-year-old woman with a 2.2 cm-sized sub-epithelial tumor. The lesion showing cardiac location, smooth margin, lower attenuation on non-enhanced image (33 HU, < 43 HU), homogeneous enhancement, and absence of enlarged lymph node. A score of 2 was assigned. Postoperative pathological diagnosis is leiomyoma. **c, d** CT images of a 32-year-old man with a 2.8 cm-

sized sub-epithelial tumor. The lesion showing non-cardial location, smooth margin, higher attenuation on non-enhanced image (54 HU), homogeneous enhancement, and absence of enlarged lymph node. A score of 2 was assigned. Postoperative pathological diagnosis is schwannoma

of CT in small gastric SETs, necrosis was observed in nine of 34 GISTs, whereas in only one of 22 non-GISTs (schwannoma + leiomyoma) [20]. Furthermore, CT findings including necrosis and heterogeneous enhancement were also found to be associated with risk stratifications previously [21]; this gave us an indication that these imaging features had the potential not only in distinguishing between GISTs and non-GISTs but also between high- and low-risk GISTs.

Attenuation on unenhanced images was another CT feature of significance between gastric GISTs and non-GISTs with a cut-off value of 43 HU, and GISTs demonstrate lower attenuation than non-GISTs in the present series. However, we have not retrieved any literature in which CT value at non-enhanced phase of gastric GISTs and other type of SETs

were compared. Thus, the certainty and pathological basis of this finding may need further study.

In the present study, non-cardial location was determined to be a significant characteristic of GISTs more than of non-GISTs, and none of the 51 GISTs were found located at cardia. This finding was in line with a previous study regarding the CT findings of ectopic pancreas, GISTs, and leiomyoma, two out of the 33 GISTs were identified in the gastric cardia, and on the contrary, six out of seven leiomyomas located at cardia [9]. In our series, older age (> 49 years) was more often observed in patients with GISTs than in non-GISTs, which has been established previously. In an epidemiologic study of GISTs, the author found that annual incidence of GISTs increased with age and peaking among 70–79 years [22]. With regard to LN, similar to our findings, the previous

studies reported that peri-lesion reactive enlarged LN was usually associated with gastric schwannoma [10, 23]. In contrary, no enlarged LN was observed in any GISTs in our series.

Based on the findings of the primary analyses, a simple and practical scoring method has been established. When being tested in a validation population, the scoring method achieved very high sensitivity and NPV for identifying GISTs. Accuracy (92%) of the present scoring method is a little higher than that of a previous study, in which Choi et al. used a five-point confidence scale to differentiate GISTs from non-GISTs and got accuracies from 87 to 90% (104/120 and 108/120 for two readers, respectively) [10]. Moreover, to optimize the practical applicability of the method in daily work, straightforward and routine imaging features as well as their simple accounting were emphasized in our work; hence, our scoring method seems to be more objective and practical than the approach of Choi et al. In addition, given the very high sensitivity and NPV, our method allows for detecting all gastric GISTs while safely excluding some non-GISTs from patients with gastric SETs, thereby may spare a number of patients from unnecessary surgery.

Of note, no significant difference was found in distribution of dynamic enhancement pattern between GISTs and non-GISTs in the primary analyses data set, and it is another finding that we want to discuss. This result could be explained by the common histopathology of these tumors which lead to a progressive enhancement: amount of fibrous stroma, smooth muscle tissue, and collagenous or myxoid change [13, 19, 23, 24]. Based on this finding, multi-phasic enhanced-CT scan cannot provide useful information for disease distinguishing, pre- and venous phase enhanced image may be enough, and thus, arterial- and delayed-phased scanning can be avoided from the CT protocol for gastric SETs.

The present study has several limitations. First, the retrospective design and exclusion of SETs' patients who did not underwent surgical resection can lead to a certain selection bias, which may have contributed to the perfect diagnostic accuracy in our series. Second, the small-sized study population may weaken the generalizability of our results. Therefore, further multi-center studies of larger sized, less-biased sample are needed to verify the reliability of the present findings and scoring system.

Conclusions

In summary, GISTs of the stomach have special CT features that differ from non-GISTs. With a simple and practical scoring method based on the combination of the significant CT and clinical features, gastric GISTs may be accurately differentiated from non-GISTs.

Acknowledgements This study was supported by grants from the National Natural Science Foundation of China (no. 81701656) and the Key Research and Development Project of Shandong Province, China (no. 2018GSF118153).

Compliance with ethical standards

Conflict of interest The authors declare no conflicts of interest.

Ethical standards All procedures followed were in accordance with the ethical standards of the responsible committee on human experimentation (institutional and national) and with the Helsinki Declaration of 1964 and later versions. This study was approved by local institutional review board from the two hospitals and informed consent was waived according to the retrospective design.

References

1. Doyle LA, Hornick JL. Mesenchymal tumors of the gastrointestinal tract other than GIST. *Surg Pathol Clin*. 2013;6(3):425–73.
2. Koo DH, Ryu MH, Kim KM, et al. Asian consensus guidelines for the diagnosis and management of gastrointestinal stromal tumor. *Cancer Res Treat*. 2016;48(4):1155–66.
3. Miyazaki Y, Nakajima K, Kurokawa Y, et al. Clinical significance of surgery for gastric submucosal tumours with size enlargement during watchful waiting period. *Eur J Cancer*. 2013;49(12):2681–8.
4. Koizumi S, Kida M, Yamauchi H, et al. Clinical implications of doubling time of gastrointestinal submucosal tumors. *World J Gastroenterol*. 2016;22(45):10015–23.
5. Barajas-Gamboa JS, Acosta G, Savides TJ, et al. Laparo-endoscopic transgastric resection of gastric submucosal tumors. *Surg Endosc*. 2015;29(8):2149–57.
6. O'Riordan D, Levine MS, Yeager BA. Complete healing of ulceration within a gastric leiomyoma. *Gastrointest Radiol*. 1985;10(1):47–9.
7. Cai MY, Xu JX, Zhou PH, et al. Endoscopic resection for gastric schwannoma with long-term outcomes. *Surg Endosc*. 2016;30(9):3994–4000.
8. Kang JH, Lim JS, Kim JH, et al. Role of EUS and MDCT in the diagnosis of gastric submucosal tumors according to the revised pathologic concept of gastrointestinal stromal tumors. *Eur Radiol*. 2009;19(4):924–34.
9. Kim JY, Lee JM, Kim KW, et al. Ectopic pancreas: CT findings with emphasis on differentiation from small gastrointestinal stromal tumor and leiomyoma. *Radiology*. 2009;252(1):92–100.
10. Choi YR, Kim SH, Kim SA, et al. Differentiation of large (≥ 5 cm) gastrointestinal stromal tumors from benign subepithelial tumors in the stomach: radiologists' performance using CT. *Eur J Radiol*. 2014;83(2):250–60.
11. Wozniak A, Rutkowski P, Schoffski P, et al. Tumor genotype is an independent prognostic factor in primary gastrointestinal stromal tumors of gastric origin: a european multicenter analysis based on ConticaGIST. *Clin Cancer Res*. 2014;20(23):6105–16.
12. Fujiwara S, Nakajima K, Nishida T, et al. Gastric schwannomas revisited: has precise preoperative diagnosis become feasible? *Gastric Cancer*. 2013;16(3):318–23.
13. Voltaggio L, Murray R, Lasota J, et al. Gastric schwannoma: a clinicopathologic study of 51 cases and critical review of the literature. *Hum Pathol*. 2012;43(5):650–9.

14. Iavarone M, Piscaglia F, Vavassori S, et al. Contrast enhanced CT-scan to diagnose intrahepatic cholangiocarcinoma in patients with cirrhosis. *J Hepatol.* 2013;58(6):1188–93.
15. Miettinen M, Sobin LH, Lasota J. Gastrointestinal stromal tumors of the stomach: a clinicopathologic, immunohistochemical, and molecular genetic study of 1765 cases with long-term follow-up. *Am J Surg Pathol.* 2005;29(1):52–68.
16. Tanaka J, Oshima T, Hori K, et al. Small gastrointestinal stromal tumor of the stomach showing rapid growth and early metastasis to the liver. *Dig Endosc.* 2010;22(4):354–6.
17. Novitsky YW, Kercher KW, Sing RF, et al. Long-term outcomes of laparoscopic resection of gastric gastrointestinal stromal tumors. *Ann Surg.* 2006;243(6):738–45 (**discussion 745–7**).
18. Choi JW, Choi D, Kim KM, et al. Small submucosal tumors of the stomach: differentiation of gastric schwannoma from gastrointestinal stromal tumor with CT. *Korean J Radiol.* 2012;13(4):425–33.
19. Hong HS, Ha HK, Won HJ, et al. Gastric schwannomas: radiological features with endoscopic and pathological correlation. *Clin Radiol.* 2008;63(5):536–42.
20. Hur BY, Kim SH, Choi JY, et al. Gastroduodenal glomus tumors: differentiation from other subepithelial lesions based on dynamic contrast-enhanced CT findings. *AJR Am J Roentgenol.* 2011;197(6):1351–9.
21. Zhou C, Duan X, Zhang X, et al. Predictive features of CT for risk stratifications in patients with primary gastrointestinal stromal tumour. *Eur Radiol.* 2016;26(9):3086–93.
22. Ma GL, Murphy JD, Martinez ME, et al. Epidemiology of gastrointestinal stromal tumors in the era of histology codes: results of a population-based study. *Cancer Epidemiol Biomark Prev.* 2015;24(1):298–302.
23. Ji JS, Lu CY, Mao WB, et al. Gastric schwannoma: CT findings and clinicopathologic correlation. *Abdom Imaging.* 2015;40(5):1164–9.
24. Layfield LJ, Wallander ML. Diagnosis of gastrointestinal stromal tumors from minute specimens: cytomorphology, immunohistochemistry, and molecular diagnostic findings. *Diagn Cytopathol.* 2012;40(6):484–90.